SHOCK WAVES IN A SHALLOW RESERVOIR

L. S. Kozachenko and B. D. Khristoforov

We report here some 1956 measurements of parameters of shock waves produced in water by underwater explosions of spherical trotyl charges in reservoirs $H_* = 1$, 2, 4, and 12 charge radii in depth and having an air-saturated sandy bottom.

1. We denote by H, h, and R, respectively, the charge depth, the measurement point, and the distance from the charge to the measurement point, expressed in units of the charge radius R_0; θ (sec /m) and τ (sec/m) are, respectively, the exponential-decay constant and the time for which the shock wave is effective, divided by R_0.

During an explosion in an unbounded liquid a shock wave has an exponential shape, and its maximum pressure p_1, time constant θ, and specific impulse i are given by [1]

$$p_1 = \frac{14700}{R^{1.13}} \text{ kg/cm}^2, \qquad \theta = 0.85 \cdot 10^{-3} R^{0.25} \text{ sec/m},$$
$$I = \frac{i}{R_0} = \frac{1}{R_0} \int_0^{6.6\theta} p(t)\, dt = 153 \cdot 10^3 R^{-0.89} \text{ kg} \cdot \text{sec/m}^3. \tag{1.1}$$

Equations (1.1) hold in the range $12 \leq R \leq 200$. During an explosion in a real reservoir the free surface and bottom will significantly affect the shock-wave parameters. In the acoustic approximation the effect of the free surface reduces to one of changing the specific momentum of the shock wave and the time for which it is effective. In this case we have, far from the center of the explosion,

$$\tau = 2\frac{Hh}{a_0 R}, \qquad I = \frac{1}{R_0} \int_0^{\tau} p(t)\, dt \tag{1.2}$$

where a_0 is the sound velocity in water. The effect of the bottom in this approximation reduces to one of forming the reflected wave and wave of seismic origin, due to refraction of longitudinal and transverse waves from the bottom into the water.

It was shown in [2-4] that the acoustic approximation cannot be used to calculate shock-wave parameters for the case of an explosion near the free surface or bottom of a reservoir. In this case nonlinear effects significantly influence the nature of the interaction between the shock wave and the boundary surfaces. The pressure dependences of the sound and front velocities must therefore be taken into account in the equations. The free surface reduces the pressure at the front and increases the time for which the wave is effective in comparison with the values calculated from Eqs. (1.1) and (1.2). A rarefaction wave arises far from a charge which explodes near the bottom of the reservoir; the interaction of this wave with the direct wave should lead to the same effects as are found during an explosion near the free surface. During an explosion in a shallow reservoir the parameters of the wave field in the water depend significantly on the nature of the combined effects of the bottom and free surface on the direct wave. Because of the complexity of this phenomenon, we have carried out an experimental study of the parameters of a shock wave set up in water during an explosion in a shallow reservoir.

2. The experiments were carried out in a reservoir 87 m long and 3 m deep having an air-saturated sandy bottom 20 m wide in the level part. The soil density and sound velocity are, respectively, $\rho_0 = 1.95$

Moscow. Translated from Zhurnal Prikladnoi Mekhaniki i Tekhnicheskoi Fiziki, No. 4, pp. 165-171, July-August, 1970. Original article submitted December 15, 1969.

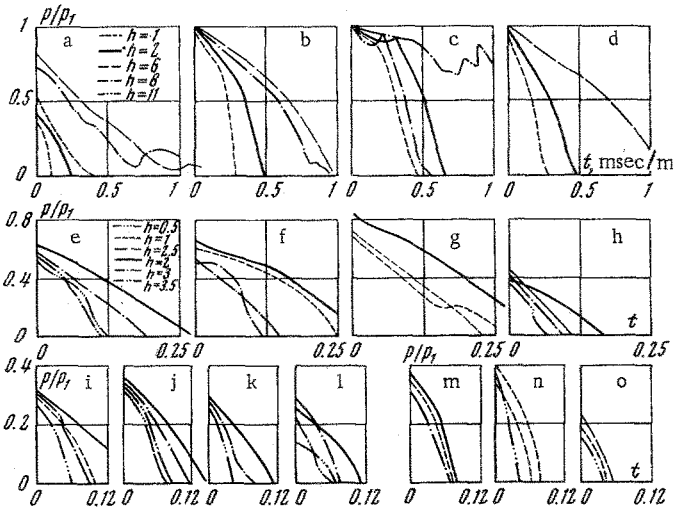

Fig. 1. Shock-wave profiles for the parameter values (H_*, H, R): a) 12, 1, 60; b) 12, 6, 60; c) 12, 8, 30; d) 12, 4, 30; e) 4, 1, 30; f) 4, 2, 30; g) 4, 3, 30; h) 4, 3, 60; i) 4, 2, 60; j) 4, 1, 60; k) 4, 3, 90; l) 4, 1, 90; m) 4, 2, 120; n) 2, 1, 30; o) 2, 1, 60.

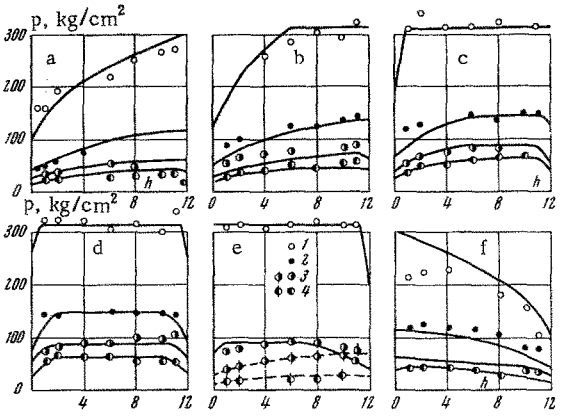

Fig. 2

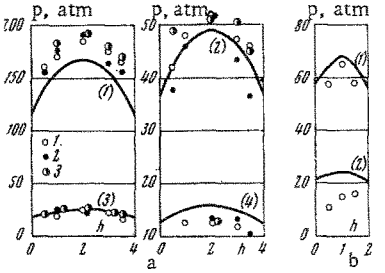

Fig. 3

Fig. 2. The reservoir depth is $H_*=12$. a-f) H=1, 2, 4, 6, 8, 11, respectively; dashed curves in Fig. 2e) H=0. There are vertical bars through the experimental points corresponding to this case. 1-4) R=30, 60, 90, 120, respectively.

Fig. 3. The p (h) dependence at the shock-wave front in reservoirs of depth $H_*=4$ and 2. R=30 (1); 60 (2); 90 (3); 120 (4). 1-3) H=1, 2, 3, respectively.

g/cm^3 and $c_1=270$ m/sec; the density of the individual grains of sand is $\rho_{01}=2.65$ g/cm^3, and the volume air concentration in the soil is $\varepsilon\sim10^{-3}$. The explosions were carried out at relative reservoir depths of $H_*=1$, 2, 4, and 12. The shock-wave parameters were measured by tourmaline pressure pickups having a sensitive-element diameter of 3-6 mm; the parameters were then recorded on PID-9 piezoelectric pressure gauges [5]. The shock-wave measurements were carried out at relative distances of R=30, 60, 90, and 120 from the center of the explosion at various charge depths H and various pickup depths h. The experimental results are shown in Figs. 1-6.

3. Figure 1 shows experimental time dependences of the pressure in shock waves for explosions in reservoirs of depths $H_*=12$, 4, and 2 for various relative distances R from the charge, various explosion depths H, and various measurement points h.

The parameters of the p (t) curves depend strongly not only on the charge position and measurement point but also on the reservoir depth. In a reservoir of depth $H_*=12$ and with $H\geq6$ (Figs. 1b and 1c), the

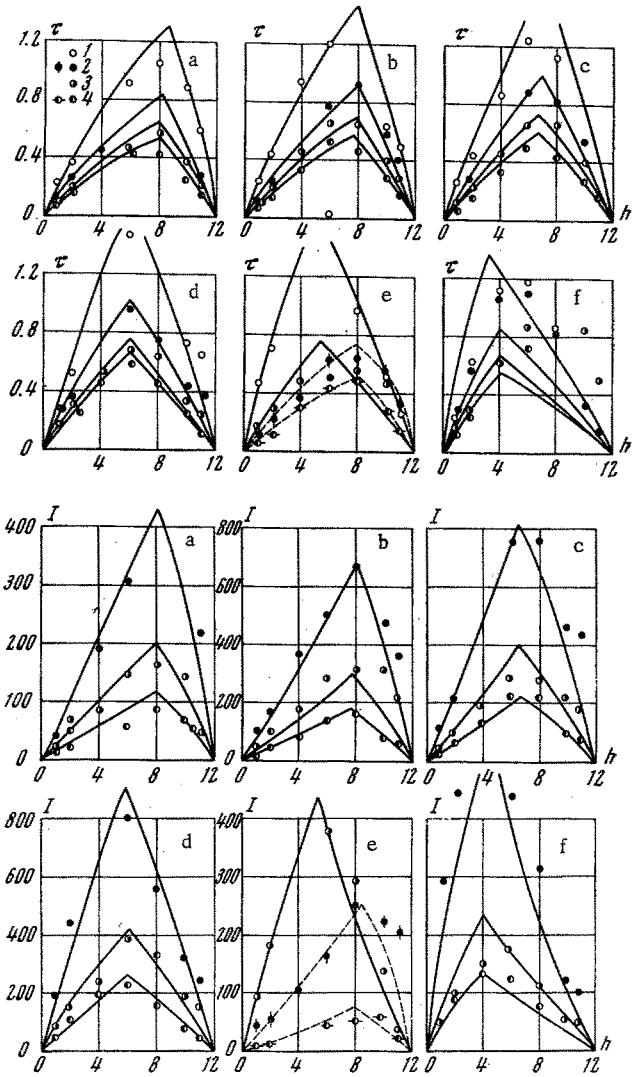

Fig. 4. The τ (h) and I (h) dependences in a reservoir of depth $H_* = 12$. a-f) Explosions at depth H = 1, 2, 4, 6, 8, 11, respectively; dashed dependences in Fig. 4e) explosion at H = 0. Lines are drawn through the experimental points for this case. 1-4) R = 30, 60, 90, 120, respectively.

p (t) dependence near the front is nearly exponential, while that at the end of the wave is nearly parabolic. The pressure at the front is equal to that given by Eq. (1.1) for an explosion in an unbounded liquid ($p/p_1 = 1$); this corresponds to regular wave reflection from the bottom and free surface [2, 3].

For the explosion at H = 8, the oscillograms show reflected compression waves followed by a rarefaction zone; this follows from the parabolic form of the p (t) curve behind the front of the reflected wave. For H < 6 (Figs. 1a and 1d), the wave has a profile (over nearly the entire range of distances studied) which consists of two parabolic segments. In this case we have $p/p_1 < 1$, which corresponds to an irregular interaction with the free surface [2, 3]. Pickups at the bottom of the reservoir detect lengthy perturbations behind the direct wave, which may be called "bottom waves" (Fig. 1a).

For explosions in the $H_* = 4$ reservoir and for all H values, the wave is nearly parabolic with a front pressure $p < p_1$. Bottom and reflected waves are not observed in this case. As the measurement point approaches the bottom or free surface, the wave parameters decrease. The maximum parameters are observed at half the reservoir depth. For $H_* = 2$, the wave shapes are similar to those observed in the preceding case, but the parameters are much lower (Figs. 1n and 1o).

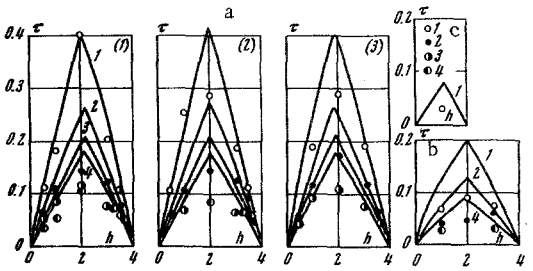

Fig. 5. The τ (h) dependence in reservoirs of depths $H_*=4$, 2, 1 (a-c, respectively). 1-4) R=30, 60, 90, 120, respectively. H= 1 (1); 2 (2); 3 (3).

Figure 2 shows the experimental dependences of the maximum pressure on the depth h of the measurement point for various R and H and for $H_*=12$.

In an explosion in the upper half of the reservoir, the front pressure increases with increasing h to a value characteristic of an explosion in an unbounded liquid. Within the experimental error, the front pressure remains constant with further increases in h, equal to $p_1=314$, 144, 93, and 64 kg/cm^2, respectively, for R=30, 60, 90, and 120.

In a charge explosion in the middle of the reservoir, with H=6, the maximum pressure is independent of h at all distances studied. In an explosion near the bottom the front pressure is minimal near the bottom, increasing with distance from the bottom. This is shown particularly clearly in Fig. 2f (H=11), where the p (h) dependence is similar to the corresponding dependence for H=1 (Fig. 2a), with the depth h reckoned from the bottom.

In a reservoir with $H_*=12$, and for an explosion near one of the boundary surfaces, the front pressure thus depends strongly on the distances from these surfaces to the charge; the boundaries have a greater effect on the front pressure as R increases.

Figures 3a and 3b show the experimental front pressure for explosions in reservoirs of depth $H_*=$ 4 and 2, respectively. Within the experimental scatter the maximum pressure during explosions in shallow reservoirs does not depend on H. The maximum front pressure is reached at half the reservoir depth at all distances from the charge; as the measurement point approaches one of the boundary surfaces, this pressure decreases. As the reservoir depth is reduced, the front pressure decreases, if the other determining parameters are held constant. With R=30 and $H_*=2$ and 1, e.g., the pressure is less by factors of 5 and 15, respectively, than in an explosion in an unbounded liquid.

Figure 4 shows τ (h) and I (h) dependences for an explosion in a reservoir of depth $H_*=12$ for the entire R and H ranges. As the measurement point approaches the bottom or the free surface, the effective time of the shock wave and its specific impulse decrease.

In the explosion in the middle of the reservoir, with H=6, the maximum τ and I are found at half the reservoir depth. As the charge is brought nearer the free surface or the bottom, the measurement points at which the maximum τ and I are found move toward the bottom and free surface, respectively. Similar τ (h) and I (h) dependences can be easily found from an estimate of the range over which the boundary surfaces affect the shock wave.

Figures 5 and 6 show the measured time for which the shock wave is effective and the specific impulse of the shock wave in reservoirs of depth $H_*=4$, 2, and 1. The maximum τ and I are found at half the reservoir depth for all H. As the measurement point is brought nearer the bottom or free surface, τ and I decrease, tending toward zero at these surfaces. The τ (h) and I (h) curves are nearly symmetric about the plane passing through the center of the reservoir parallel to the boundary surface. The τ and I values decrease with decreasing H_* and are essentially independent of H.

4. These experimental results show that the parameters of shock waves produced by explosions near a free surface differ significantly from those in an unbounded liquid. The interaction of a shock wave with a free surface during an explosion near the surface was described in [3] with an account of nonlinear effects. Semiempirical equations were also given there for the parameters of the shock wave, whose form was selected on the basis of an analysis of the solution given in [2] and the experimental data of [3]. The maximum pressure during an explosion near a free surface is

$$\frac{p}{p_1}=\frac{p^1}{p_1}\left\{1+\frac{h\left[(p_1/p^1)^3-1\right]}{4R\alpha^*(1-1.2\alpha/\alpha^*)^4}\right\}^{1/3}=K_1$$

$$p^1/p_1=(1+\alpha/\alpha^*)^2/4,\qquad \alpha\approx H/R,\qquad (4.1)$$

$$\alpha^*=[(n+1)\,p_1/2Bn]^{1/2}$$

$$B=3050\ \text{kg/cm}^2,\quad n=7.15$$

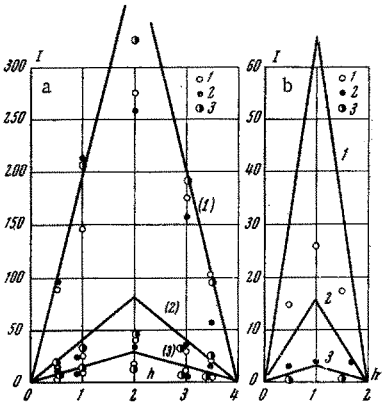

Fig. 6. The I (h) dependence in a reservoir of depth: a) $H_* = 4$. Here 1-3 correspond to H = 1, 2, 3, respectively, and (1), (2), (3) correspond to R = 30, 60, 90, respectively; b) $H_* = 2$ and H = 1. Here 1-3 correspond to R = 30, 60, 120, respectively.

Equation (4.1) holds for $K_1 \leq 1$; for $K_1 \geq 1$, we have $p = p_1$. For H = 0, p_1 can be calculated from Eq. (1.1) with half the given charge. The time for which the shock wave is effective and the specific impulse of the shock wave are

$$\tau = 2\frac{Hh}{a_0 R} l_1, \qquad l_1 = 0.55\left(\frac{\alpha^*}{\alpha} + 1\right) - \frac{h}{6H}\left(1 - \frac{h}{R}\right) \tag{4.2}$$

We see that $I = 0.5 p\tau$ for $H \leq 1$ and $I = 0.6 p\tau$ for $H \geq 2$. Equations (4.2) hold for $l_1 \geq 1$; for $l_1 < 1$, the calculation is made on the basis of the acoustic-approximation equations (1.2).

Analysis of the experimental data shows that the reservoir bottom has effects on the shock-wave parameters analogous to those of the free surface. This type of interaction between the shock wave and the bottom must be governed by the characteristics of the soil. Air-saturated and water-saturated sand can be assumed to be a low-velocity bottom, since the velocities c_1 and c_2 of longitudinal and transverse waves, respectively, in it are lower than the sound velocity in water: $a_0 > c_1 > c_2$. We can derive the soil's p (ρ) dependence, which governs the interaction of the shock wave with the bottom, with an account of the measured soil characteristics.

We assume that in an initial soil volume V_0 the volume concentrations of dry sand, water, and air are n_0, m_0, and ε_0, respectively. Then the initial ρ_0 and final ρ of the three-phase medium are given by

$$\rho_0 = \rho_{01} n_0 + \rho_{02} m_0 + \rho_{03}\varepsilon_0, \quad \rho = \rho_1 n + \rho_2 m + \rho_3 \varepsilon \tag{4.3}$$

where ρ_1, ρ_2, and ρ_3 are the density of the sand grains, water, and air after compression. Using Hooke's law to describe the deformation of the sand grains and the water, the Poisson adiabat for air, and the conditions

$$n_0 + m_0 + \varepsilon_0 = n + m + \varepsilon = 1, \quad \varepsilon \ll n, \; m$$

we find the following dependences for the state parameters of the three-phase soil and the parameters of the shock wave in it:

$$\frac{\rho_0}{\rho} = 1 - (p - p_0)\left(\frac{n_0}{k} + \frac{m_0}{L}\right) - \varepsilon_0\left[1 - \left(\frac{p_0}{p}\right)^{1/\gamma}\right] \tag{4.4}$$

$$c_0 = \left[\left(\frac{\partial p}{\partial \rho}\right)_s\right]^{1/2}_{p \to p_0} = \left[\rho_0\left(\frac{n_0}{k} + \frac{m_0}{L} + \frac{\varepsilon_0}{\gamma p_0}\right)\right]^{-1/2} \tag{4.5}$$

$$D = \left\{\rho_0\left(\frac{n_0}{k} + \frac{m}{L}\right) + \frac{\varepsilon_0\rho_0}{p - p_0}\left[1 - \left(\frac{p_0}{p}\right)^{1/\gamma}\right]\right\}^{-1/2} \tag{4.6}$$

$$W = \frac{p - p_0}{\rho_0}\left\{\rho_0\left(\frac{n_0}{k} + \frac{m_0}{L}\right) + \frac{\varepsilon_0\rho_0}{p - p_0}\left[1 - \left(\frac{p_0}{p}\right)^{1/\gamma}\right]\right\}^{1/2} \tag{4.7}$$

Here $K = 38 \cdot 10^{10}$ dyn/cm^2 and $L = 2.2 \cdot 10^{10}$ dyn/cm^2 are the bulk moduli of quartz and water, $\gamma = 1.4$ is the index of the air adiabat, and W and D are the mass and wave velocity of the soil.

From Eqs. (4.3) and (4.5) and from data on the density of the soil components and the velocity found in it given above, we find $n_0 = 0.576$, $m_0 = 0.424$, and $\varepsilon_0 = 10^{-3}$.

Calculations show that for normal incidence of a shock wave on a bottom having characteristics (4.4) and (4.5) at pressures below 12 atm, reflection of the rarefaction wave occurs, since the compressibility of the soil at these pressures, due primarily to air deformation in pores, is very high. At higher pressures, the compression wave is reflected, since the compressibility of the soil decreases sharply after the air-filled pores collapse. The pressure under the charge was high during the explosions in these experiments, and the compression wave was reflected from the bottom at normal incidence of the wave. Far from the charge, where the wave is incident on the bottom at an angle α, both the compression and rarefaction waves may be reflected.

Where the incident wave strikes the bottom we have

$$N\cos\alpha = N\cos\beta = D / \cos\gamma,\ p^* = p_2$$
$$u\sin\alpha = w\sin\gamma + (u_n^* - u_n)\sin\beta \tag{4.8}$$

where α, β, and γ are the angles of incidence, reflection, and refraction, respectively, between the front and the normal to the bottom. Here the asterisk denotes a parameter of the reflected wave, the n denotes a component of the mass velocity normal to the front of the reflected wave, and p_2 and w denote the pressure and mass velocity of the wave in the soil. Reflection does not occur at the incidence angle α_1 found from the equality of the components of the mass velocities in the soil and in the incident wave normal to the bottom. In this case we have

$$u\ \sin\alpha_1 = w\ \sin\gamma$$

Using (4.8), we can then show that

$$\sin\alpha_1 = \left[\frac{1-(D/N)^2}{(u/w)^2-(D/N)^2}\right]^{1/2} \tag{4.9}$$

For $\alpha > \alpha_1$, the compression wave is reflected, as can be seen from the experimental oscillograms in Fig. 1c. For $\alpha < \alpha_1$, the rarefaction wave must be reflected from the bottom. In this case the flow which is observed during an explosion near the free surface must be established at the bottom. We have carried out some calculations for the angle α_1 on the basis of Eq. (4.9) for various distances from the charge, and for the angles

$$\alpha^* = [(n+1)\,p_1 / 2Bn]^{1/2},$$

which characterize, by analogy with the interaction with the free surface, the onset of irregular reflection from the bottom [2, 3]:

$R = 30$	60	90	120
$p_1 = 314$	144	91	64
$\alpha_1 = 0.166$	0.268	0.352	0.436
$\alpha^* = 0.242$	0.164	0.129	0.112

In the distance range studied we usually have $\alpha_1 > \alpha^*$, so in a reservoir with $H_* = 12$, where cases of $\alpha > \alpha_1$ and $\alpha < \alpha_1$ are possible, a transition is observed from a first regular-reflection region (the case of compression-wave reflection) to a second regular-reflection region (reflection of the rarefaction wave, which does not overtake the front of the direct wave) and then, at $\alpha > \alpha^*$, to an irregular-reflection region (the rarefaction waves reduce the front pressure). This transition can be followed on the oscillograms. For a given H, it results in an increase in R; for given R, it results in an increase in H. In addition, the reflection conditions may change abruptly from those characteristic of the first region to those characteristic of irregular reflection, with the second regular-reflection region omitted. This occurs with R = 30, where we have $\alpha_1 < \alpha^*$. Experimentally, we observe a decrease in τ and I in the range $\alpha > \alpha_1$ as the measurement point approaches the bottom (Fig. 1c). In this case, according to the pattern described above for reflection from the bottom, a reflected shock wave arises (this wave is visible on the oscillograms). However, it is followed by a rarefaction wave, whose explanation lies outside the scope of this paper. In this case, for the distances studied in the $H_* = 12$ reservoir, the time for which the direct wave is effective is therefore governed in a first approximation by the time at which the wave reflected from the bottom arrives.

In the reservoirs of depth $H \leq 4$, the shock wave at all measurement points is in the region of irregular reflection from the bottom and from the free surface. For angles of incidence on the bottom corresponding to the formation of a reflected rarefaction wave, we can describe the parameters of the shock wave by equations analogous to Eqs. (4.1) and (4.2). Here we can assume that the flow at the bottom is analogous to that of the free surface:

$$\frac{p}{p_1} = \frac{p^1}{p_1}\left\{1 + \frac{h_1[(p_1/p)^3 - 1]}{4R\alpha^*(1 - 1.2\alpha/\alpha^*)^4}\right\}^{1/3} = K_2 \tag{4.10}$$
$$\alpha \approx H_1 / R$$

$$\tau = 2\frac{H_1 h_1}{a_0 R} l_2, \qquad l_2 = 0.55\left(\frac{\alpha^*}{\alpha} + 1\right) - \frac{h_1}{6H_1}\left(1 - \frac{h_1}{R}\right)$$
$$I = 0.5\,p\tau \text{ for } H < 1,\ \alpha = 0.6\,p\tau \text{ for } H \geq 2, \tag{4.11}$$

where H_1 and h_1 are the distances of the charge and pickup from the reservoir bottom. The same restrictions hold for Eqs. (4.10) and (4.11) as for Eqs. (4.1) and (4.2).

In a shallow reservoir, in which the bottom and free surface affect the direct wave simultaneously, the maximum shock-wave pressure is

$$p = p_1 K_1 K_2' \text{for} \quad K_1 \leqslant 1, \; K_2 \leqslant 1 \tag{4.12}$$

where K_1 and K_2 are given by Eqs. (4.1) and (4.10). If the K_1 or K_2 values calculated from Eqs. (4.1) and (4.10) turn out to be greater than 1, we should substitute $K=1$ into Eq. (4.12).

In a shallow reservoir with a sandy bottom, τ is equal to the lesser of the values given by Eqs. (4.2) and (4.11).

Figures 2-6 show, along with the experimental data, curves calculated from Eqs. (4.2), (4.11), and (4.12). These curves are seen to be in satisfactory agreement with the experimental data. For the explosions in the reservoirs with $H_*=2$ and 1, the experimental points are slightly below these curves; this result indicates the presence of a complex wave field, formed by the superposition of waves multiply reflected from the reservoir boundaries. (The equations shown here for the parameters take into account the interaction of the direct wave with only those waves reflected once from the reservoir boundaries.) Nevertheless, these equations give the parameters of shock waves in shallow reservoirs with low-velocity bottoms with an accuracy suitable for practical purposes.

The authors thank A. G. Ryabinin, A. I. Stanilovskii, K. I. Baryshev, L. N. Gal'perin, and K. K. Chernetskii for participating in this study.

LITERATURE CITED

1. R. H. Cole, Underwater Explosions, Dover (1965).
2. A. A. Grib, A. G. Ryabinin, and S. A. Khristianovich, "Reflection of a planar shock wave from a free surface," Prikl. Matem. i Mekhan., 20, No. 3 (1956).
3. B. D. Khristoforov, "Interaction of a shock wave in water with a free surface," Zh. Prikl. Mekhan. i Tekh. Fiz., No. 1 (1961).
4. B. D. Khristoforov, "Experimental study of the interaction of a shock wave in water with a rigid reservoir bottom," Zh. Prikl. Mekhan. i Tekh. Fiz., No. 4 (1960).
5. A. I. Sokolik and A. I. Stanilovskii, "The PID-9 two-channel piezoelectric pressure gauge," in: Leading Practice in Science and Technology [in Russian], Izd. VINITI, Moscow (1957).